

## Revealing Structural Effects: Electrochemical Reactions of Butanols on Platinum

José L. Rodríguez, Ricardo M. Souto, Luis Fernández-Mérida, and Elena Pastor\*<sup>[a]</sup>

**Abstract:** Spectroelectrochemical studies on the reactivity of butanol isomers on Pt electrodes in perchloric acid medium led to the observation of structural effects that result from the different arrangements of atoms in the organic molecules. The use of differential electrochemical mass spectrometry (DEMS) to detect volatile products showed that all four isomers react on the electrode, though different product yields were observed for each compound. In spite of the differences in the electrochemical behaviour of the buta-

nol isomers, a series of general processes accounts for the results obtained. The formation of strongly adsorbed residues by a dehydration process leading to the formation of a C=C bond was proposed for all isomers. Electroreduction of the adsorbates produces C<sub>4</sub> and C<sub>3</sub> alkanes, and the latter reveal the existence of a fragmentation process. The C<sub>4</sub> hydro-

**Keywords:** adsorption • butanols • electrochemistry • mass spectrometry • platinum

carbons can be formed by hydrogenation of these residues and by hydrogenolysis of alcohol molecules in the bulk solution which react at the electrode with adsorbed hydrogen. On the other hand, CO<sub>2</sub> is formed during electrooxidation of the adsorbed species. Partial-oxidation products containing a carbonyl group were detected from 0.2 M solutions of 1-butanol, isobutyl alcohol and *sec*-butyl alcohol. The tertiary alcohol *tert*-butyl alcohol only reacts in its adsorbed state.

### Introduction

The electrochemical reactivity of organic compounds on noble electrodes in aqueous solution depends, among other factors, on the chemical nature of the electrode, the nature of the organic compound and the electrode potential.<sup>[1, 2]</sup> Short-chain alcohols such as methanol, ethanol and ethylene glycol are widely regarded as interesting model organic compounds for such studies, and have been the object of systematic investigations to elucidate reaction pathways and to establish their applicability as direct-combustion fuels.<sup>[3–12]</sup> In all cases, the formation of adsorbed intermediates was shown to be of paramount importance for the kinetics of the overall process, and their identification was fundamental to elucidating the mechanisms. In this respect, the introduction of novel spectroscopic techniques in the electrochemical laboratory has provided valuable information for identifying the species participating in these complex reactions.<sup>[13–18]</sup>

The extension of these studies to alcohols with longer chains has demonstrated the influence of the molecular structure on the electroreactivity of these compounds. In this

way, differences in the adsorption and reaction mechanisms were found during the investigation of primary C<sub>3</sub> alcohols with different degrees of unsaturation.<sup>[19–23]</sup> Structural effects can also be expected in molecules that only differ in the position of the functional group, owing to different inductive electronic effects and different availability of the reaction sites. 1-Propanol and 2-propanol, a primary and a secondary alcohol, respectively, are the simplest examples for such a situation and exhibit remarkable differences in electrochemical behaviour. On platinum electrodes, they both can be electrooxidised to yield CO<sub>2</sub> and partially oxygenated species (propanal and propionic acid from 1-propanol,<sup>[20]</sup> and acetone from 2-propanol<sup>[24–26]</sup>). These alcohols also show significant differences in their electroreduction reactions, as the position of the OH group in the primary alcohol strongly favours rupture of the C<sub>3</sub> chain, a process that does not occur when the hydroxyl group is attached to the central atom as in 2-propanol. These observations were supported by differential electrochemical mass spectrometry (DEMS),<sup>[20, 26]</sup> Fourier transform infrared spectroscopy (FTIRS)<sup>[20, 26]</sup> and radio-tracer<sup>[27]</sup> experiments.

Herein we give consideration to the aliphatic C<sub>4</sub> alcohols, which introduce the smallest tertiary alcohol, namely, *tert*-butyl alcohol. Several studies have been published regarding the behaviour of butanol isomers on different noble metal electrodes, though they mainly deal with electrochemical investigations on platinum.<sup>[28–30]</sup> It was concluded that the primary alcohols are the most reactive on platinum, though

[a] Prof. Dr. E. Pastor, Prof. Dr. J. L. Rodríguez, Prof. Dr. R. M. Souto, Prof. Dr. L. Fernández-Mérida  
Departamento de Química Física  
Universidad de La Laguna  
38071 La Laguna, Tenerife (Spain)  
Fax: (+34) 922-318002  
E-mail: epastor@ull.es

they produced strongly poisoning intermediates, whereas for the secondary isomer the reactivity was lower. Finally, no response was observed for the tertiary alcohol at room temperature.<sup>[29, 30, 33]</sup> Unfortunately, all these studies relied exclusively on the analysis of electrochemical data, and no spectroscopic techniques which could help in understanding the structural effects responsible for the differences in reactivity were employed. The only exception is a recent paper on an FTIRS study on the electroadsorption and reactivity of 1-butanol on platinum in acidic solution.<sup>[34]</sup> The authors proposed a reaction scheme in which the molecule undergoes dissociative adsorption in parallel to its oxidation to butanoic acid and CO<sub>2</sub>. But even for this alcohol, some statements are still tentative, such as the proposed formation of propane and 1-butanal, which could not be experimentally demonstrated by FTIRS.<sup>[34]</sup>

We therefore undertook a systematic study on the electro-reactivity of 1-butanol and its isomers on platinum in acid solution using DEMS<sup>[35]</sup> to detect gaseous and volatile products. A DEMS study of the electrochemical behaviour of the isolated adsorbates from butanol isomers on platinum, obtained by using a flow-cell procedure, is currently underway and is the subject of a future publication.<sup>[36]</sup>

## Experimental Section

**Experimental details:** Differential electrochemical mass spectrometry (DEMS) was used for on-line detection of volatile products. Details of the method are described elsewhere.<sup>[35, 37]</sup> In brief, a porous layer of platinum metal deposited on a Teflon membrane forms the interface between the electrochemical cell and the ion source of the mass spectrometer. The counterelectrode was a platinum wire, and the reference electrode was a reversible hydrogen electrode (RHE) in aqueous 0.1M HClO<sub>4</sub>. Simultaneously to the cyclic voltammograms (CVs), the ion current for selected mass to charge ratios ( $m/z$ ) was recorded as mass spectrometric cyclic voltammograms (MSCVs).

All solutions were prepared from Millipore MilliQ\* plus water (18.2 M $\Omega$ cm), and high-purity chemicals (Fluka) to ensure that each of the butanol isomers was not contaminated with any of the others. This was of paramount importance in the case of *tert*-butyl alcohol, which was reported in the literature to be electrochemically unreactive at room temperature.<sup>[29, 30, 33]</sup> Chromatographic analysis of a solution of *tert*-butyl alcohol showed it to be free from traces of the other isomers. 0.1M HClO<sub>4</sub> was used as base solution, and the concentration of butanol isomers was fixed at 0.2M. Solutions were carefully deaerated with 99.998% argon. All measurements were performed at room temperature.

The working electrode was activated in 0.1M HClO<sub>4</sub> by applying repetitive potential cycles at 0.01 Vs<sup>-1</sup> between 0.01 and 1.50 V until a reproducible voltammogram was obtained. The real area (15–25 cm<sup>2</sup>) was measured through the voltammetric charge within the hydrogen potential range for platinum.<sup>[38]</sup> After electrode activation in the base electrolyte, exchange with the alcohol-containing solution was performed at a potential in the double-layer region of the platinum electrode. The second potential cycle is shown in all cases. Each  $m/z$  ratio was recorded at least three times. Reproducible CVs and MSCVs were obtained.

**The platinum surface and product assignment:** The identification of the oxidation and reduction products generated at the platinum electrode, after recording appropriate  $m/z$  values with DEMS, requires knowledge of any changes in the state of the metal surface with the applied potential.

The CV for a platinum surface in 0.1M HClO<sub>4</sub> shows three potential regions:

1) The “hydrogen region” (0.01–0.40 V), which is characterised by the presence of adsorbed hydrogen on the electrode surface. The features observed in the voltammetric curve correspond to the adsorption/

desorption of hydrogen atoms with different energies. At  $E < 0.10$  V hydrogen evolution occurs.

2) The “platinum oxide region”: at  $E > 0.75$  V a platinum oxide layer starts to form with increasingly positive potential, and is subsequently electro-reduced during the reverse sweep with the development of a peak centred at 0.77 V.

3) The “double-layer region”: in this potential range (0.40–0.75 V during the positive run, narrower in the cathodic sweep), neither H<sub>ad</sub> nor O<sub>ad</sub> species are present at the surface.

The presence of oxygen at  $E > 0.75$  V favours the formation of oxidation products, whereas at  $E < 0.40$  V, the reduction process prevails, that is, oxidation reactions are not expected to occur at potentials at which the surface is mainly covered with hydrogen. This fact must be considered in the interpretation of the mass-spectrometric curves obtained with DEMS.

Platinum is a good catalyst for the oxidation of organic compounds to CO<sub>2</sub>. Thus, carbon dioxide was observed with methanol,<sup>[3]</sup> ethanol<sup>[4–10]</sup> and other alcohols<sup>[20–22, 24–26]</sup> including 1-butanol.<sup>[34]</sup> On the other hand, the formation of hydrocarbons from these alcohols at potentials in the hydrogen region was established many years ago by gas chromatographic analysis.<sup>[39]</sup> Therefore, oxidation and reduction processes take place on platinum in different potential ranges.

In accordance with these general statements, the identification of the products from the analysis of the recorded MSCVs must be performed carefully. Thus, even the same value of  $m/z$  could be assigned to different fragments of different molecules, depending on the potential region considered. Previous electrochemical data on the nature of the reduction and oxidation products that were obtained with other techniques can be used to elucidate the nature of these compounds, though the application of DEMS introduces a clear advantage: the potential dependence of their production can also be established.

Fragmentation patterns from reduction and oxidation products, as well as those from the electroactive organic compound (the alcohol in our case), must be considered for the interpretation of each MSCV. The criteria for the selection of the  $m/z$  values to be recorded are: 1) the most intense peaks corresponding to the fragmentation patterns of the predicted compounds and 2) peaks which do not overlap with fragments from other products. If fragments from different compounds contribute to the same  $m/z$  signal, then the ion-current curves should be interpreted after comparison of the potential dependencies and ion-current intensities of various MSCVs. This procedure has been extensively applied for DEMS analysis.<sup>[3, 19–23, 35, 40–46]</sup>

## Results

**Primary alcohols:** Typical cyclic voltammograms for a Pt electrode in 0.1M HClO<sub>4</sub> containing 0.2M 1-butanol or 0.2M isobutyl alcohol are depicted in Figures 1A and 2A (solid line), respectively. They show two features during the positive potential scan, the main one centred at 1.25 V, with a previous contribution around 0.90 V. The threshold potential for the oxidation of the alcohols (0.70 V) is below the onset of platinum oxide formation (cf. the CV measured in the base electrolyte, as depicted in Figures 1A and 2A, dotted lines). During the reverse potential scan, a new anodic current was observed in the cyclic voltammograms in the potential range 0.80–0.40 V. This feature is apparent as soon as the platinum surface becomes free of oxide. In this scan, a cathodic contribution is recorded at potentials below 0.20 V, which is more pronounced for 1-butanol.

Despite similar currents being measured for the two primary isomers in the hydrogen region, as well as for the electrooxidation occurring at 0.90 V in the positive sweep, the faradic current for the peak centred at 1.28 V in the case of 1-butanol is about half that of isobutyl alcohol (cf. Figures 1A and 2A).

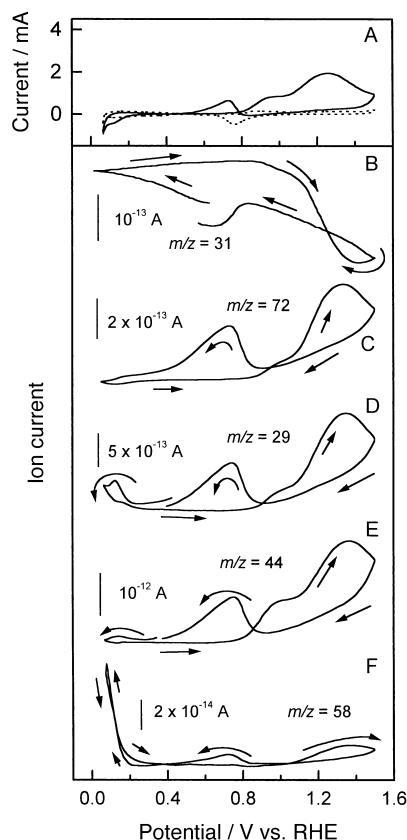


Figure 1. A) Cyclic voltammogram of a Pt electrode in 0.2M 1-butanol + 0.1M  $\text{HClO}_4$ ,  $\nu = 0.01 \text{ V s}^{-1}$ , real area =  $17.7 \text{ cm}^2$  (—); CV in the base electrolyte (---). MSCVs for B)  $m/z = 31$  (1-butanol), C)  $m/z = 72$  (1-butanol), D)  $m/z = 29$  (1-butanol, propane and butane), E)  $m/z = 44$  ( $\text{CO}_2$ , 1-butanol and propane) and F)  $m/z = 58$  (butane).

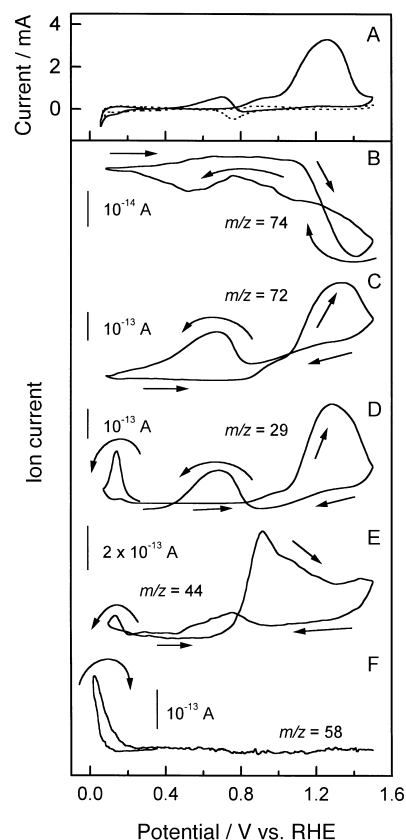


Figure 2. A) Cyclic voltammogram of a Pt electrode in 0.2M isobutyl alcohol + 0.1M  $\text{HClO}_4$ ,  $\nu = 0.01 \text{ V s}^{-1}$ , real area =  $18.1 \text{ cm}^2$  (—); CV in the base electrolyte (---). MSCVs for B)  $m/z = 74$  (isobutyl alcohol), C)  $m/z = 72$  (isobutanol), D)  $m/z = 29$  (isobutanol and propane), E)  $m/z = 44$  ( $\text{CO}_2$  and propane) and F)  $m/z = 58$  (isobutane).

Potential-dependent mass signals obtained simultaneously with the voltammetric runs for several  $m/z$  values are shown in Figures 1B–F and 2B–F. The consumption of the two primary alcohols could be monitored by means of the potential dependence of the  $m/z = 31$  and  $m/z = 74$  signals (Figures 1B and 2B, respectively). The ion current for  $m/z = 31$  is related to the main fragment of 1-butanol ( $[\text{CH}_2\text{OH}]^+$ ), whereas  $m/z = 74$  corresponds to the radical cation of isobutyl alcohol  $[(\text{CH}_3)_2\text{CHCH}_2\text{OH}]^+$ . The two  $m/z$  ratios are quite stable during the positive scan up to 1.50 V in both the hydrogen and double-layer ranges of platinum, followed by a decrease at  $E > 0.80 \text{ V}$ . The consumption of the alcohols is thus observed in the potential ranges for the two electrooxidation features apparent in the corresponding CVs (cf. Figures 1A and 2A). At  $E > 1.40 \text{ V}$  and after potential reversal at 1.50 V, effective blockage of the electrode occurs due to the platinum oxide layer formed on the metal, which allows for a gradual recovery of the alcohol concentration around the electrode. Nevertheless, a decrease in the mass signals is again observed at  $E < 0.80 \text{ V}$  during the negative sweep, which closely matches the anodic current in the CVs.

The electrooxidation products of the primary butanols were identified from the potential dependence of the signals for  $m/z = 72$ , 29 and 44. The mass to charge ratio  $m/z = 72$  corresponds to formation of the radical cation of the butanal resulting from the oxidation of the corresponding butanol

( $[\text{CH}_3\text{CH}_2\text{CH}_2\text{CHO}]^{+\bullet}$  for 1-butanol and  $[(\text{CH}_3)_2\text{CHCHO}]^{+\bullet}$  for isobutanol). This ion current increases when the positive potential scan exceeds 0.70 V and reaches a maximum at around 1.30 V with a shoulder at about 0.97 V. Accordingly, the regions of consumption described above correlate with the maxima for the formation of the corresponding aldehydes in Figures 1C and 2C for 1-butanol and isobutyl alcohol, respectively.

The production of butanals was confirmed by the signal for  $m/z = 29$  (Figures 1D and 2D), which corresponds to the characteristic  $[\text{CHO}]^+$  fragment of aldehydes. Comparison of the mass spectrometric cyclic voltammograms (MSCVs) measured for  $m/z = 72$  and  $m/z = 29$  in the two solutions clearly reveals the same potential dependence at  $E > 0.25 \text{ V}$ . The contributions observed at potentials below 0.20 V (cf. Figures 1D and 2D) have to be assigned to the electroreduction of the alcohol (see below). Support for this idea is provided by inspecting the MSCVs for  $m/z = 72$  (Figures 1C and 2C), which show no features in the hydrogen region.

On the other hand, the ion current for  $m/z = 44$  could correspond, in principle, to the formation of  $\text{CO}_2$  ( $[\text{CO}_2]^{+\bullet}$ ) as the second electrooxidation product. This is the case for isobutyl alcohol (see Figure 2E). The onset for this signal is observed during the positive run at around 0.60 V and increases steadily until a maximum value is reached at 0.90 V. Then, a decay of the signal is observed at  $E > 0.90 \text{ V}$ .

After potential reversal at 1.50 V,  $\text{CO}_2$  production is strongly inhibited until the Pt oxide layer is partially reduced. Then, the ion current increases again to define a new  $\text{CO}_2$  contribution with a maximum at 0.75 V.

In contrast, the  $m/z = 44$  signal recorded in the solution containing 1-butanol (Figure 1E) shows the same features as the signal for  $m/z = 72$  (Figure 1C). The discrepancy arises from the contribution to the mass to charge ratio  $m/z = 44$  observed in the fragmentation patterns of 1-butanol.<sup>[40]</sup> According to the literature, the presence of this ion current in the spectrum is due to McLafferty rearrangement in the ionisation chamber of the mass spectrometer,<sup>[48]</sup> which in the case of 1-butanol leads to the fragment  $[\text{CH}_2=\text{CHOH}]^{+\bullet}$ . This rearrangement can take place in this case because it is characteristic of molecules with an H atom in a  $\gamma$ -position to an unsaturated group.<sup>[48]</sup> However, the signal for  $m/z = 44$  in Figure 1E depicts a higher ion current around 0.95 V than that for  $m/z = 72$ . Therefore, it seems that  $\text{CO}_2$  is also formed in this potential region, and its contribution to the signal for  $m/z = 44$  overlaps with that from 1-butanol at the same mass to charge ratio. Additional support for this interpretation was obtained during oxidative stripping of the adsorbed residues of 1-butanol from platinum after a flow-cell experiment.<sup>[36]</sup> As shown in Figure 3A,B, after adsorption at 0.15 V and electrolyte replacement, the residues formed from this isomer are oxidised to  $\text{CO}_2$  with a peak at around 1.07 V (Figure 3B). In the adsorption experiment, the signal for  $m/z = 44$  is exclusively assigned to  $\text{CO}_2$ , as no potential dependence is observed for  $m/z = 72$ .

On the basis of these results it is concluded that, whereas in the case of isobutyl alcohol the  $m/z = 44$  signal is exclusively due to the production of carbon dioxide, the corresponding signal in the case of 1-butanol corresponds to the contribution of butanal and  $\text{CO}_2$  formation. This is the reason for the major difference in the ion current scales in Figures 1E and 2E.

As mentioned before, electroreduction of the alcohols occurs at  $E < 0.20$  V. For the assignment of the reduction products, the MSCVs for  $m/z = 30$ , 29, 28, 15 and 14 were recorded in addition to those shown in Figures 1 and 2. By

considering the fragmentation patterns of various hydrocarbons, it was established that saturated  $\text{C}_4$  and  $\text{C}_3$  hydrocarbons are the main products in this process (other compounds could be formed in traces). As expected, different potential dependencies were observed for the mass signals assigned to each hydrocarbon.

The MSCVs for  $m/z = 44$  in this potential region, associated with the radical cation  $[\text{CH}_3\text{CH}_2\text{CH}_3]^{+\bullet}$  of propane, increase and develop a maximum at 0.12–0.14 V during the negative sweep (see Figures 1E and 2E). The production of butane and isobutane can be monitored by means of the MSCVs for  $m/z = 58$  in Figures 1F and 2F, assigned to the radical cation of butane  $[\text{CH}_3\text{CH}_2\text{CH}_2\text{CH}_3]^{+\bullet}$  in the case of 1-butanol, and to the radical cation of isobutane  $[(\text{CH}_3)_2\text{CHCH}_3]^{+\bullet}$  in the case of isobutyl alcohol. The maximum in this signal is observed at the cathodic potential limit of the scan. The difference in the ion-current intensities in Figures 1F and 2F is explained in terms of the different contributions of the radical cation  $[\text{C}_4\text{H}_{10}]^{+\bullet}$  to the fragmentation patterns of butane (about 15 %) and isobutane (about 3 %).

Both propane and butane contribute to the signal for  $m/z = 29$  at potentials below 0.15 V by means of the fragment  $[\text{CH}_3\text{CH}_2]^{+\bullet}$  in Figure 1D, whereas only propane is responsible for the response in Figure 2D (the contributions of butane and isobutane to this ion current are ca. 40 and 4 %, respectively).

It is noteworthy that the shape of the curves for the signals related to propane ( $m/z = 44$ , 29) is similar to those obtained from the isolated adsorbates,<sup>[36]</sup> whereas some changes are observed in the ion currents associated with the  $\text{C}_4$  hydrocarbon. This result confirms that alcohol molecules in the bulk contribute to the signal  $m/z = 58$ .

Some additional features are evident in the MSCV for  $m/z = 58$  at  $E > 0.50$  V in the solution containing 1-butanol (see Figure 1F). They are certainly not due to butane formation. This could be an indication that traces of propanal are formed during the electrooxidation process, which would correspond to the radical cation  $[\text{CH}_3\text{CH}_2\text{CHO}]^{+\bullet}$ . However, the shape of the mass voltammogram in this potential range resembles that recorded for 1-butanol ( $m/z = 72$ , Figure 1C). This similarity suggests that the contributions result from the natural content of  $^{13}\text{C}$  in the fragment  $[\text{CH}_2\text{CH}_2\text{CHO}]^{+\bullet}$  from butanal.

**Secondary alcohol:** The CV of a platinum electrode in 0.2 M *sec*-butyl alcohol and 0.1 M  $\text{HClO}_4$  is shown in Figure 4A (solid line). An anodic current is already observed in the double-layer potential range of platinum during the positive potential sweep, with a feature centred at 0.70 V, which is followed by a second feature at 1.30 V in the oxide region. In the reverse scan, a sharp peak is followed by a hump at 0.64 V in the cyclic voltammogram at potentials

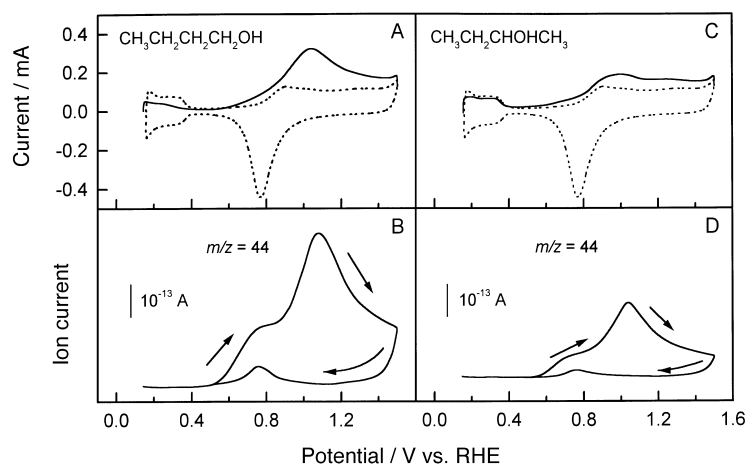


Figure 3. Electrooxidation of the residues formed on a Pt electrode after adsorption from a base solution containing 0.2 M of the butanol, followed by electrolyte exchange with 0.1 M  $\text{HClO}_4$ ;  $E_{\text{ad}} = 0.15$  V,  $v = 0.01$  V  $\text{s}^{-1}$ , real area = 17.7  $\text{cm}^2$ . A) CV and B) MSCV for  $m/z = 44$  ( $\text{CO}_2$ ) after adsorption of 1-butanol. C) CV and D) MSCV for  $m/z = 44$  ( $\text{CO}_2$ ) after adsorption of *sec*-butyl alcohol. CV in the base electrolyte (---).

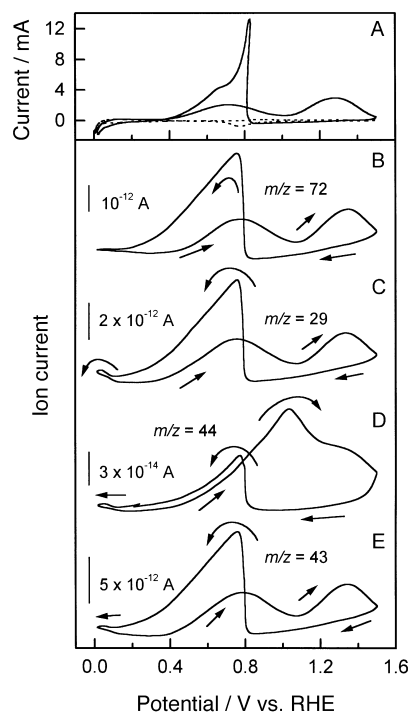


Figure 4. A) Cyclic voltammogram of a Pt electrode in 0.2 M *sec*-butyl alcohol + 0.1 M  $\text{HClO}_4$ ,  $v = 0.01 \text{ V s}^{-1}$ , real area =  $24.6 \text{ cm}^2$  (—); CV in the base electrolyte (---). MSCVs for B)  $m/z = 72$  (butanone), C)  $m/z = 29$  (butanone, propane and butane), D)  $m/z = 44$  ( $\text{CO}_2$ , butanone and propane) and E)  $m/z = 43$  (propane and butane).

below 0.83 V. The electrooxidation in the double-layer potential range during the positive run and the sharp anodic current increase in the negative potential excursion are characteristic voltammetric features for the secondary alcohol, as they were not observed for either 1-butanol or isobutyl alcohol (cf. Figures 1A and 2A).

Mass signals recorded during the voltammetric scan for selected  $m/z$  values are shown in Figures 4B–E. The MSCVs for  $m/z = 72$ , 29 and 43 exhibit the same features at  $E > 0.20 \text{ V}$ , and therefore seem to correspond to the same product. In this case, these signals are assigned to the radical cation and the fragments  $[\text{CH}_3\text{CH}_2]^+$  and  $[\text{CH}_3\text{CO}]^+$  from butanone, respectively. During the positive run, the onset for butanone is observed around 0.30 V (see Figure 4B,C,E). Two ion-current contributions of approximately the same height are centred at 0.75 and 1.35 V. In the reverse sweep, butanone production is strongly inhibited until the platinum oxide layer is partially reduced, and then the ion currents increase sharply and attain a maximum at 0.76 V. The height of the signal at 0.76 V in the mass spectrometric curves is twice as high as those recorded during the preceding potential scan. Therefore, the peak in the CV for this scan direction is related to the formation of the ketone.

The ion current for  $m/z = 44$  shows a different behaviour and therefore must be related to a new electrooxidation product. This compound is  $\text{CO}_2$ , as was the case for the primary alcohols. This MSCV increases steadily during the positive scan from 0.30 V and reaches a maximum at 1.03 V, which is followed by a slow decay with a hump at approximately 1.35 V. The hump is not observed during the oxidative

stripping of the adsorbates formed from *sec*-butyl alcohol on platinum (see Figure 3C,D). Moreover, the onset of  $\text{CO}_2$  production in Figure 3D is 0.50 V, that is, more positive than in Figure 4D. This is explained in terms of a contribution to the  $m/z = 44$  signal from the fragmentation of butanone.<sup>[40]</sup> During the reverse scan, the signal shows an electrooxidation feature around 0.77 V. The ion intensity in this potential range is higher than that observed in Figure 3D. Therefore, also in this region the contribution of butanone to  $m/z = 44$  is apparent.

The features at  $E < 0.20 \text{ V}$  in the signals for  $m/z = 29$ , 44 and 43 (Figure 4C–E) are less pronounced than in Figures 1 and 2, but it must be emphasized that the intensity of the signals at  $E > 0.20 \text{ V}$  is higher in the case of *sec*-butyl alcohol, and, therefore, a different scale was employed in the plot. The curves show the same potential dependence in the hydrogen region, with a maximum at 0.04 V in the negative potential sweep. This behaviour differs from those of the primary alcohols. These contributions are explained in terms of the formation of propane and butane, as in the case of 1-butanol.

**Tertiary alcohol:** The reactivity of *tert*-butyl alcohol is very low at room temperature, as can be deduced by inspection of the voltammogram shown in Figure 5A. The existence of various peaks in the hydrogen-adsorption region of platinum and a well-defined double-layer potential range are still easily recognisable in the CV. However, during the positive potential scan, a broad contribution is observed in the potential region of platinum oxide. In the reverse scan, a slight decrease

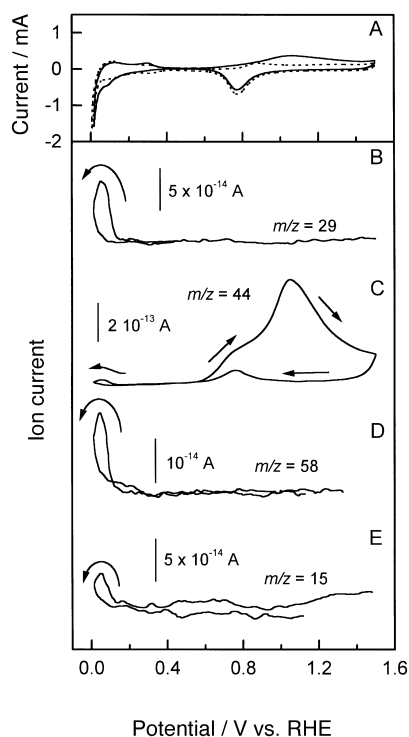


Figure 5. A) Cyclic voltammogram of a Pt electrode in 0.2 M *tert*-butyl alcohol + 0.1 M  $\text{HClO}_4$ ,  $v = 0.01 \text{ V s}^{-1}$ , real area =  $22.3 \text{ cm}^2$  (—); CV in the base electrolyte (---). MSCVs for B)  $m/z = 29$  (propane), C)  $m/z = 44$  ( $\text{CO}_2$  and propane), D)  $m/z = 58$  (isobutane) and E)  $m/z = 15$  (isobutane, propane and methane).

in the charge covered under the voltammetric peak due to the electroreduction of platinum oxide is recorded, as well as a significant increase in the cathodic charge measured in the  $H_{ad}$  region.

Furthermore, the occurrence of electrochemical reactions at the platinum electrode in the acidic solution containing *tert*-butyl alcohol is unambiguously established from DEMS measurements. Several potential-dependent signals were found, which demonstrate that the tertiary alcohol undergoes both electrooxidation and electroreduction processes. The mass signals recorded for *tert*-butyl alcohol are shown in the MSCVs of Figure 5B–D.

The electrooxidation of *tert*-butyl alcohol is represented by the production of  $CO_2$  at  $E > 0.55$  V, as monitored by the MSCV for  $m/z = 44$  (Figure 4B), since no other species was detected by checking different  $m/z$  values. This agrees with the observation that the shape of the ion-current curve for  $m/z = 44$  closely follows that of the CV in this potential range. In the positive scan, the yield of  $CO_2$  attains a maximum at 1.05 V with a shoulder at 0.75 V. Its production continues during the negative potential sweep after most of the platinum oxide is reduced, and displays a feature around 0.76 V.

The formation of three reduction products at  $E < 0.20$  V was established from the MSCVs for  $m/z = 29$ , 44, 58 and 15 (Figure 5B–E). These signals are attributed to propane ( $m/z = 29$ , 44, 15) and isobutane ( $m/z = 58$ , 15), analogously to the reduction products of isobutyl alcohol. However, the intensity for the ratio  $m/z = 15$  is higher than can be expected from the fragmentation patterns for propane and isobutane.<sup>[40]</sup> Thus, it appears to be plausible that a third hydrocarbon is formed in this potential region. Accordingly, we regard methane as another product in the process (see Discussion). All these ion currents show a peak at 0.05 V in the negative run, in contrast to the primary alcohols.

## Discussion

**Preliminary considerations:** The electrochemical reactivity of dissolved butanols on platinum in perchloric acid solution was confirmed to depend on the molecular structure of the organic substance. The position of the hydroxyl group in the aliphatic chain determines the electrochemical reactions and the potential range in which they occur. The use of DEMS to detect volatile products allowed a better analysis of the influence of the molecular structure. It was of crucial importance in studying the electroreactivity of *tert*-butyl alcohol, which was previously regarded as unreactive on platinum electrodes in sulfuric acid solution at room temperature.<sup>[29,30, 33]</sup>

To facilitate comparison of the electrochemical reactivity of the four butanol isomers on platinum electrodes, the results described in the previous section are summarised as follows:

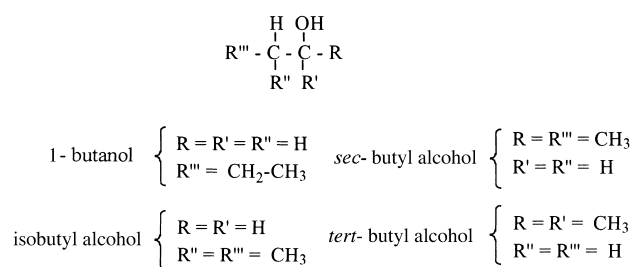
- 1) Stable cyclic voltammograms show that all the four alcohols are oxidised during the positive potential scan. The onset potential for the oxidation process was 0.30 V for *sec*-butyl alcohol, whereas for the other isomers this reaction commences at 0.70 V. Two anodic features were observed for 1-butanol, isobutyl alcohol and *sec*-butyl

alcohol, but only one broad feature for *tert*-butyl alcohol (cf. Figures 1A, 2A, 4A and 5A). Except for *tert*-butyl alcohol, the oxidation of these molecules also takes place during the negative potential scan when the Pt oxide layer is partially reduced. The highest reactivity was observed for *sec*-butyl alcohol (especially during the negative potential sweep), and the lowest for *tert*-butyl alcohol.

- 2) The anodic contributions observed in the CVs correlate directly with the consumption of the alcohols on the electrode, as can be monitored, for example, by means of the potential dependence of the MSCVs measured for  $m/z = 31$  in the case of 1-butanol (see Figure 1B), and for  $m/z = 74$  in the case of isobutyl alcohol (Figure 2B).
- 3) All four molecules undergo electrooxidation to  $CO_2$  (see Figures 1E, 2E, 4D and 5C), although partially oxidised products (the corresponding aldehydes or ketone; see Figures 1C, 2C, and 4B) are produced, except for *tert*-butyl alcohol. Importantly, the formation of the corresponding carboxylic acid during the electrooxidation of the primary alcohols, with the aldehyde as reaction intermediate, could not be excluded on the basis of our measurements. This uncertainty originates from the significant differences in volatility between each aldehyde and the corresponding carboxylic acid, the former being the only volatile species suitable for detection in the mass spectrometer, while the carboxylate species diffuse in the solution instead.
- 4)  $CO_2$  was identified as the main electrooxidation product in the potential range covered by the current peak centred around 0.90 V. The formation of aldehydes occurs at more positive potentials and is responsible for the current at  $E > 0.90$  V and during the reverse scan in Figures 1 and 2. The production of butanone from *sec*-butyl alcohol is observed for  $E > 0.30$  V in Figure 4, that is, in the double-layer region, prior to oxidation to  $CO_2$ . Electrooxidation processes occurred mainly in parallel to the adsorption of oxygen on platinum, though they become progressively hindered by the platinum oxide layer that develops on the surface of the electrode, and can only continue on the oxide-free platinum surface during the negative voltammetric scan.
- 5)  $CO_2$  originates from adsorbates, as was confirmed by oxidative stripping of the adsorbates formed at 0.15 V on platinum in a flow-cell (Figure 3).
- 6) Electroreduction of the butanol isomers takes place in the hydrogen-adsorption potential range of platinum, with the production of the corresponding butane isomer and propane. Therefore, a dissociative reaction leading to the formation of the latter occurs in all cases.

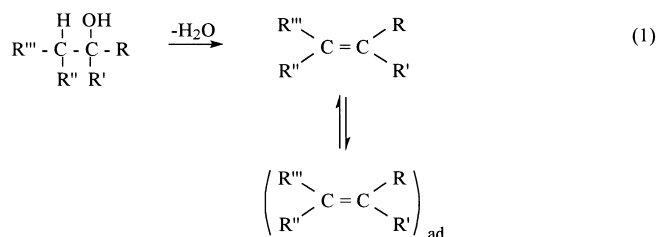
**Possible electrode reactions:** Despite the significant differences observed in the reactivity of the isomers, which result in different product yields for each of them, they share some general trends, too, as summarised above. Therefore, it is possible to explain all these observations by considering a general reaction scheme for the butanol isomers, which must take into account the reaction pathways responsible for the formation of the different products. To facilitate the discussion, a general formula for the butanol isomers is presented,

from which the four isomers can be derived by identifying the groups R, R', R'', and R'''.



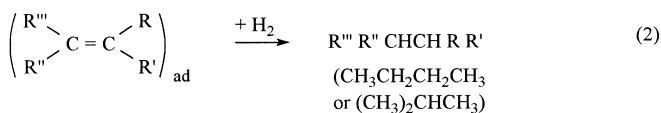
For the complete description of the electrochemical characteristics of butanol isomers reacting on platinum electrodes in acidic media, six reaction steps are proposed.

**Dehydration:** The interaction of the butanol isomers in acid solution with a platinum surface must lead to the formation of physisorbed molecular species that probably are weakly bound to the metal surface. Next, dehydration of these species leads to the formation of strongly adsorbed intermediates containing a C=C bond [Eq. (1)].



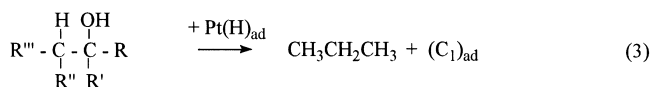
The existence of such intermediates is indicated by FTIR measurements, as was shown for 1-butanol in the potential range between 0.25 and 0.60 V<sup>[34]</sup>. The only requirement for this reaction to take place is that the organic compound must contain a hydrogen atom  $\alpha$  to the OH group. As this is the case for all four butanol isomers, this reaction pathway is proposed for all the butanols.

**Hydrogenation:** Addition of hydrogen to the C=C bond in the adsorbates formed in reaction (1) leads to the formation of the corresponding butanes (butane in the cases of 1-butanol and sec-butyl alcohol, and isobutane for isobutyl alcohol and tert-butyl alcohol). This process [Eq. (2)] explains the MSCVs recorded for  $m/z=58$  and occurs in the potential range for hydrogen evolution on platinum.



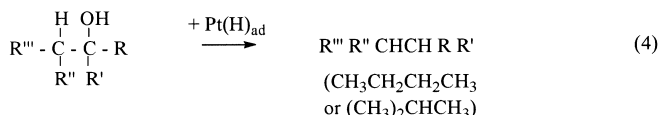
**Fragmentation:** The detection of propane in the potential range for hydrogen adsorption on platinum, as given by the mass ratio  $m/z=29$ , indicates that the C=C bond in the adsorbates can be broken to give C<sub>3</sub> and C<sub>1</sub> species. The

detection of methane in addition to propane was only possible in the case of *tert*-butyl alcohol and was monitored by means of the signal for  $m/z=15$ . This may indicate that C<sub>1</sub> species remain adsorbed on the electrode surface in the case of the other butanol isomers [Eq. (3)].

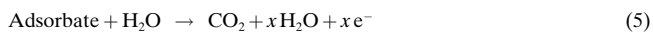


This C<sub>1</sub> adsorbate is assigned as CO<sub>ad</sub> for 1-butanol, as detected in FTIR studies,<sup>[34]</sup> and given the observed voltammetric and DEMS behaviours, seems to be the same for isobutyl alcohol and *tert*-butyl alcohol, too. In the case of *sec*-butyl alcohol, the formation of propane can only be explained if a rearrangement occurs during adsorption of the alcohol in the hydrogen region or on the surface, as the expected hydrocarbons would be methane and ethane. However, no evidence for the formation of these compounds instead of propane was found.

**Hydrogenolysis:** The reaction between the alcohol molecules in the bulk solution and the hydrogen adsorbed on the electrode may also lead to the formation of the C<sub>4</sub> alkane. This process was already proposed to describe the electrochemical reactivity of other alcohols on platinum in acidic media<sup>[8, 20, 26]</sup>. Accordingly, DEMS results reported here suggest that this process is responsible for the higher yields of hydrocarbons from 1-butanol and isobutyl alcohol, that is, the reaction is favoured for the primary alcohols [Eq. (4)].

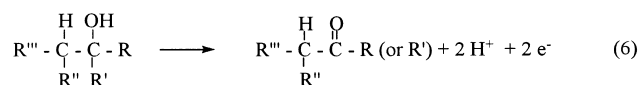


**Complete oxidation:** The oxidation of the adsorbed residues at  $E > 0.50$  V produces CO<sub>2</sub>. The participation of residues in this reaction was further confirmed by the experiments conducted in a flow-cell. The oxidative stripping of the butanol adsorbates from the platinum electrode can be described by Equation (5).



**Partial oxidation:** During the electrooxidation of the primary and secondary alcohols, namely, 1-butanol, isobutyl alcohol and *sec*-butyl alcohol, the corresponding aldehydes and the ketone were detected by DEMS ( $m/z=72$ ) as reaction products in addition to CO<sub>2</sub>. Partial oxidation is supported by FTIRS data for the electrooxidation of 1-butanol.<sup>[34]</sup> The spectra show the loss of CO (band at ca. 2050 cm<sup>-1</sup>), simultaneous with the formation of CO<sub>2</sub> (feature at 2345 cm<sup>-1</sup>) and the appearance of a band at 1712 cm<sup>-1</sup> related to the formation of a carbonyl compound,<sup>[34]</sup> which was interpreted as the formation of the corresponding acid, whereas the formation of the aldehyde could not be determined.

On the other hand, as the formation of compounds containing the carbonyl group is only observed for the primary and secondary alcohols, but not for *tert*-butyl alcohol, we must assume that one of the groups R or R' must be a hydrogen atom for this reaction to occur. The corresponding stoichiometric reaction can be expressed by Equation (6).



During the positive potential scan, the onset potential for this process is 0.30 V for the secondary alcohol (*sec*-butyl alcohol) and 0.70 V for the primary isomers (1-butanol and isobutyl alcohol). Moreover, in the reverse scan a strong reactivation of the surface is recorded for *sec*-butyl alcohol once it is free from oxide. According to these results, it is concluded that this process occurs more easily for secondary alcohols (similar results were obtained for 1-propanol<sup>[20]</sup> and 2-propanol<sup>[24–26]</sup>). This observation also suggests that the surface is strongly poisoned in the case of 1-butanol and isobutyl alcohol, and only when the oxidation of the residues commences can bulk molecules undergo further partial oxidation. For *sec*-butyl alcohol, the blockage is lower, that is, a smaller amount of adsorbed species is present on the surface during the potentiodynamic experiment, and the partial oxidation already occurs at potentials in the double-layer region.

## Conclusion

The existence of structural effects in the electroreactivity of organic compounds has been demonstrated by using electrochemical mass spectrometry (DEMS) for the detection of the volatile products formed during the electrochemical reactions of butanol isomers on platinum in acidic media. In this way, the influence of the molecular structure could be analysed.

The kinetics and the mechanism of the processes strongly depend on the number of H atoms  $\alpha$  to the OH group. All four isomers, respectively bearing two, one or no  $\alpha$ -H atoms, can be chemisorbed on platinum in a dehydration process that produces adsorbates with a C=C bond, which interact with the electrode through their  $\pi$ -electron density.

On the other hand, potential cycling in the hydrogen-potential range leads to the cleavage of the molecules, their relative fraction depending on the nature of the isomer, and probably on the potential at which they were adsorbed. This last possibility cannot be established from our studies performed in solutions containing the organic compounds, and therefore must be investigated on the adsorbates formed in a flow-cell, which is currently under way in our laboratory. In this process, propane is formed. Additionally, the existence of hydrogen adsorbed on the electrode allows cathodic stripping, at potentials below 0.20 V, of the adsorbates formed in the dehydrogenation reaction, which produces the corresponding butane isomer.

Another reaction route is the oxidation of the alcohols to partially oxidised compounds, that is, aldehydes and probably

carboxylic acids (though these compounds could not be confirmed in this work) are products in the oxidation of the primary alcohols, whereas butanone is formed from *sec*-butyl alcohol. *tert*-Butyl alcohol does not undergo this reaction; this means that a hydrogen atom must be bound to the carbon atom bearing the OH group. Furthermore, this process is mainly maintained by the species in solution and cannot take place with the residues. Although this conclusion must be confirmed by studies on the reactivity of adsorbed species, some evidence is provided by the previous observation that CO<sub>2</sub> was the only oxidation product formed from the adsorbates of 1-propanol<sup>[20]</sup> and 2-propanol,<sup>[26]</sup> whereas partially oxidised compounds were detected when these C<sub>3</sub> alcohols were present in the solution in contact with the platinum electrode.<sup>[20, 26]</sup>

Finally, the residues formed from the four butanol isomers undergo oxidative stripping to CO<sub>2</sub>. These adsorbed species are responsible for the strong poisoning effects observed for the primary alcohols on platinum, which result in the absence of electrochemical activity in the double-layer potential range. Only after oxidation of some of the adsorbed species is the electrode activated again, and the partial-oxidation pathway operates simultaneously. However, the surface must be less blocked by the adsorbates from *sec*-butyl alcohol, as this compound undergoes oxidation in the double-layer region prior to the oxidation of the residues to CO<sub>2</sub>.

## Acknowledgement

This work was supported by the Dirección General de Investigación (Ministerio de Ciencia y Tecnología of Spain) under Project No. BQU2000-0864, and the Gobierno Autónomo de Canarias under Project No. PI1999/070.

- [1] *Adsorption of Molecules at Metal Electrodes* (Eds.: J. Lipkowski, P. N. Ross), VCH, Weinheim, **1992**.
- [2] *Structure of Electrified Interfaces* (Eds.: J. Lipkowski, P. N. Ross), VCH, Weinheim, **1993**.
- [3] T. Iwasita in *Electrochemical Science and Engineering, Vol. 1* (Eds.: E. Gerischer, C. W. Tobias), VCH, Weinheim, **1990**, pp. 127–170, and references therein.
- [4] J. Willsau, J. Heitbaum, *J. Electroanal. Chem.* **1985**, 194, 27–35.
- [5] B. Bittins-Cattaneo, S. Wilhelm, E. Cattaneo, H. W. Buschmann, W. Vieltisch, *Ber. Bunsenges. Phys. Chem.* **1988**, 92, 1210–1218.
- [6] L.-W. H. Leung, S.-C. Chang, M. J. Weaver, *J. Electroanal. Chem.* **1989**, 266, 317–336.
- [7] M. Shibata, N. Furuya, M. Watanabe, *J. Electroanal. Chem.* **1989**, 267, 163–170.
- [8] T. Iwasita, E. Pastor, *Electrochim. Acta* **1994**, 39, 531–537; T. Iwasita, E. Pastor, *Electrochim. Acta* **1994**, 39, 547–551.
- [9] U. Schmiemann, U. Müller, H. Baltruschat, *Electrochim. Acta* **1995**, 40, 99–107.
- [10] J. Shin, W. J. Tornquist, C. Korzeniewski, C. S. Hoaglund, *Surf. Sci.* **1996**, 364, 122–130.
- [11] W. Hauffe, J. Heitbaum, *Electrochim. Acta* **1978**, 23, 299–304.
- [12] F. Kadirgan, B. Beden, C. Lamy, *J. Electroanal. Chem.* **1983**, 143, 135–152.
- [13] *Spectroelectrochemistry, Theory and Practice* (Ed.: R. J. Gale), Plenum, New York, **1988**.
- [14] *Spectroscopic and Diffraction Techniques in Interfacial Electrochemistry* (Eds.: C. Gutiérrez and C. Melendres), Kluwer, Dordrecht, **1990**.

- [15] *Techniques for Characterization of Electrodes and Electrochemical Processes* (Eds.: R. Varma, J. R. Selman), The Electrochemical Society/Wiley, New York, **1991**.
- [16] *Electrochemical Interfaces* (Ed.: H. D. Abruña), VCH, New York, **1991**.
- [17] *Synchrotron Techniques in Interfacial Electrochemistry* (Eds.: C. A. Melendres, A. Tadjeddine), Kluwer, Dordrecht, **1994**.
- [18] *Physical Electrochemistry: Principles, Methods, and Applications* (Ed.: I. Rubinstein), Marcel Dekker, New York, **1995**.
- [19] E. Pastor, M. C. Arévalo, S. González, A. J. Arvia, *Electrochim. Acta* **1991**, 36, 2003–2013.
- [20] E. Pastor, S. Wasmus, T. Iwasita, M. C. Arévalo, S. González, A. J. Arvia, *J. Electroanal. Chem.* **1993**, 350, 97–116.
- [21] E. Pastor, S. Wasmus, T. Iwasita, M. C. Arévalo, S. González, A. J. Arvia, *J. Electroanal. Chem.* **1993**, 353, 81–100.
- [22] E. Pastor, S. Wasmus, T. Iwasita, M. C. Arévalo, S. González, A. J. Arvia, *J. Electroanal. Chem.* **1994**, 371, 167–177.
- [23] M. C. Arévalo, J. L. Rodríguez, E. Pastor, *J. Electroanal. Chem.* **2001**, 505, 62–71.
- [24] L. W. H. Leung, M. Weaver, *Langmuir* **1990**, 6, 323–333.
- [25] S. G. Sun, Y. Lin, *J. Electroanal. Chem.* **1994**, 375, 401–404.
- [26] E. Pastor, S. González, A. J. Arvia, *J. Electroanal. Chem.* **1995**, 395, 233–242.
- [27] V. E. Kazarinov, S. V. Dolidze, *Elektrokhimiya* **1973**, 9, 1183–1187.
- [28] E. Sokolova, *Electrochim. Acta* **1975**, 20, 323–330.
- [29] S. N. Raicheva, M. V. Christov, E. I. Sokolova, *Electrochim. Acta* **1981**, 26, 1669–1676.
- [30] D. Takky, B. Beden, J. M. Leger, C. Lamy, *J. Electroanal. Chem.* **1983**, 145, 461–466.
- [31] M. V. Christov, E. I. Sokolova, *J. Electroanal. Chem.* **1984**, 175, 183–193.
- [32] E. I. Sokolova, M. V. Christov, *J. Electroanal. Chem.* **1984**, 175, 195–205.
- [33] D. Takky, B. Beden, J.-M. Leger, C. Lamy, *J. Electroanal. Chem.* **1985**, 193, 159–173.
- [34] N.-H. Li, S.-G. Sun, *J. Electroanal. Chem.* **1997**, 436, 65–72.
- [35] B. Bittins-Cattaneo, E. Cattaneo, P. Königshoven, W. Vieltisch, in *Electroanalytical Chemistry: A Series of Advances, Vol. 17* (Ed.: A. J. Bard), Marcel Dekker, New York, **1991**, pp. 181–220.
- [36] J. L. Rodríguez, R. M. Souto, G. Pastor, E. Pastor, unpublished results.
- [37] J. L. Rodríguez, E. Pastor, V. M. Schmidt, *J. Phys. Chem. B* **1997**, 101, 4565–4574.
- [38] R. Woods in *Electroanalytical Chemistry, Vol. 9* (Ed.: A. J. Bard), Marcel Dekker, New York, **1976**, pp. 1–162.
- [39] B. I. Podlovchenko, O. A. Petry, A. N. Frumkin, H. Lal, *J. Electroanal. Chem.* **1966**, 2, 12–25.
- [40] *Atlas of Mass Spectral Data* (Eds.: E. Stenhagen, S. Abrahamsson, F. W. McLafferty), Interscience, New York, **1969**.
- [41] H. Baltruschat in *Interfacial Electrochemistry: Theory, Experiment and Application* (Ed.: A. Wieckowski), Marcel Dekker, New York, **1999**, Chapter 33, pp. 577–597.
- [42] T. Hartung, H. Baltruschat, *Langmuir* **1990**, 6, 953–957.
- [43] T. Hartung, U. Schmiemann, I. Kamphausen, H. Baltruschat, *Anal. Chem.* **1991**, 63, 44–48.
- [44] U. Schmiemann, H. Baltruschat, *J. Electroanal. Chem.* **1992**, 340, 357–363.
- [45] H. Baltruschat, U. Schmiemann, *Ber. Bunsenges. Phys. Chem.* **1993**, 97, 452–420.
- [46] U. Schmiemann, Z. Jusys, H. Baltruschat, *Electrochim. Acta* **1994**, 39, 561–576.
- [47] U. Müller, U. Schmiemann, A. Dülberg, H. Baltruschat, *Surf. Sci.* **1995**, 335, 333–342.
- [48] F. W. McLafferty, F. Turecek, *Interpretation of Mass Spectra*, University Science Books, Sausalito, California, **1993**.

Received: June 11, 2001

Revised: December 20, 2001 [F3325]